

Fabrication And Characterization Of Nickel Heterojunction Oxide Nanoparticles/Silicon

¹Ahmed N. Abd

Physics Department, Science
Faculty, University of Al-
Mustansiriyah, Baghdad, Iraq

²Reem S.Ali

Physics Department, Science
Faculty, University of Al-
Mustansiriyah, Baghdad, Iraq

³Ali A. Hussein

Chemical Department, Faculty of
Science, University of Al-
Mustansiriyah, Baghdad, Iraq

¹Corresponding author, E-mail: ahmed_naji_abd@yahoo.com

Abstract—In this study, (NiO) thin film which prepared by chemical method and deposited by drop casting technique on glass. The structural, optical and chemical analyses have been investigated. X-ray diffraction (XRD) measurements relieve that the (NiO) thin film was polycrystalline, cubic structure and there is no trace of the other material. UV-Vis measurements reveal that the energy gap of (NiO) thin film was found 1.8 eV. The Fourier Transform Infrared Spectroscopy (FTIR) spectrum of (NiO) thin film shows NiO nanoparticles had its IR peak of Ni–O stretching vibration and shifted to blue direction. Due to their quantum size effect and spherical nanostructures, the FTIR absorption of NiO nanoparticles is blue-shifted compared to that of the bulk form.

Keywords—Thin film; XRD; energy gap; drop casting.

1. Introduction

Nickel oxide (NiO) is a promising p-type semiconducting oxide material [1], [2] having a wide band gap of 3.6 eV to 4 eV [3]. It resembles NaCl structure with octahedral Ni (II) and (O₂₋) sites [4]. Due to its enormous potential applications such as, anti-ferromagnetic material [5], [6], chemical sensors [7], electrochromic devices [8], catalysts [9], dye sensitized solar cells (DSSCs) [10], it attracts the researchers attention towards it. NiO thin films were fabricated using many methods such as electron beam evaporation [11], reactive sputtering [12], plasma enhanced chemical vapour deposition [13], pulsed

laser deposition [14], spray pyrolysis [15], chemical bath deposition [16] etc. Among various methods, spray pyrolysis is one through which the films can be coated for large area. In this present work a low cost and simplified chemical method to fabricate the NiO thin films.

2. Experimental

In a typical procedure, 1.6g of Ni(NO₃)₂, (BDH Chemicals Ltd Pool England) was dissolved in 60 ml of PVP (Sigma Aldrich USA) 1WT. % and Re-distilled water was used throughout the experiment. The solution was added into a round-bottom flask with stirring. The color of the mixture was green. About 15ml of NaOH (1M) was rapidly added to the mixture, and a nanopowder suspension was formed as shown in figure 1. The suspension was kept at 80 °C for 1 h. After cooling to room temperature, the particles were separated by centrifugation and were washed with distilled water to remove any contaminations.



Fig.1: NiO freshly colloidal nanoparticles) which are prepared by chemical(left) which are prepared by chemical method and the solution(right)

Figure 2 shows that NiO colloidal nanoparticles which are prepared by chemical method are deposited by drop casting technique on glass substrate. It has been taken from the solution by pipette and then drop on glass surface only 5 drops, the particles were then dried by using heater at 80 °C , then the film is ready.

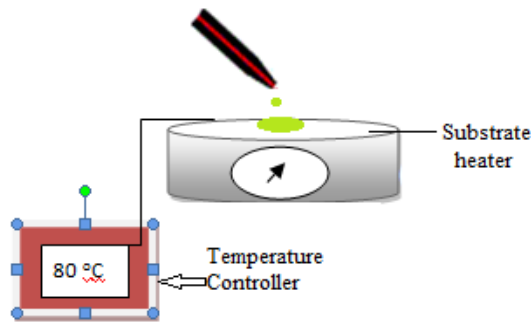


Fig.2: Schematic diagram drop casting method experimental set up.

X-ray diffractometer (XRD-6000, Shimadzu) was used to investigate the structure and crystallinity of nanoparticles. The absorption of the colloidal nanoparticles solution was measured by using UV–Vis double beam spectro-photometer (CECIL, C. 7200, France).

3. Results and discussion

The XRD diffraction patterns of synthesized NiO nanoparticles film prepared by quick chemical method is shown in Figure (3). This figure reveals three peaks at $2\theta = 37.14^\circ, 44.6^\circ$ and 63.1° corresponds to (111), (200) and (220) planes respectively which belong to NiO cubic structure (JCPDS card no.71-1179), furthermore, this figure show another peaks which agreement with the cards (JCPDS 89-7129: Ni, 14-0481: Ni₂O₃, 89-8397: NiO₂). The crystallite size (D) was calculated by using Scheerer's formula [17].

$$D = \frac{0.9\lambda}{\beta \cos\theta} \quad (1)$$

Where λ is the x-ray wavelength of CuK α source 0.154056 nm, θ is the Bragg's angle and β is the full width at half maximum (FWHM) of the diffraction peak in radians. The dislocation density (δ) and microstrain (η) values are evaluated by using the following relations [18].

$$\delta = \frac{1}{D^2} \quad (2)$$

$$\eta = \frac{\beta \cos(\theta)}{4} \quad (3)$$

The calculated grain size, microstrain and dislocation density values are presented in Table1.

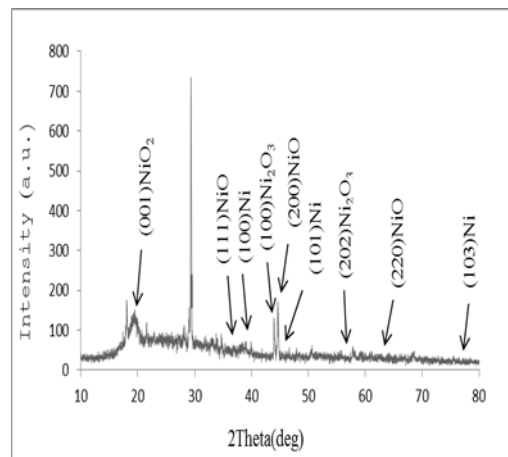


fig.3: XRD pattern of (NiO) thin film which prepared by chemical method and deposited by drop casting technique on glass

Table (1): X-Ray characterization for NiO nanoparticles

2 θ (deg)	(hkl) plane s	β (deg)	D (nm)	$\delta \times 10^4$ lines .m ⁻²	$\eta \times 10^4$ lines ⁻² .m ⁻⁴
19.36	NiO ₂ (001)	0.22	34.3	8.46	9.79
39.36	Ni (100)	0.09	81.4	1.50	3.76
43.94	Ni ₂ O ₃ (100)	0.11	63.1	2.51	4.71
44.6	NiO (200)	0.13	53.3	3.50	5.54

The microstrain and dislocation density of NiO nanoparticles films chemical reaction were around $5.54 \times 10^{-4} \text{ lines}^{-2} \cdot \text{m}^{-4}$ and $3.5 \times 10^{-4} \text{ lines} \cdot \text{m}^{-2}$ respectively.

Figure 4 shows 3D AFM image and Granularity accumulation distribution chart of NiO nanoparticles prepared by chemical method and deposited on glass substrate at 80 °C.

Substrate is well covered with NiO nanoparticles; distributed uniformly on the surface. It is obvious from this figure that the nanoparticles have small ordered particles with semispherical shape with the existence of some monopod rods. The average particle size estimated with the aid of software

was about 95 nm.

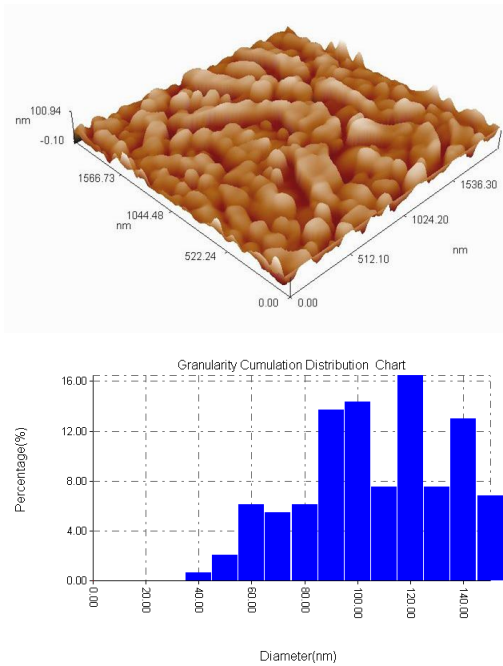


Fig. 4: 3D AFM images of NiO thin film surface and Granularity accumulation distribution chart .

Figure 5 shows the transmittance spectrum of (NiO) thin film. The data are corrected for glass transmission in UV region. Also, the figure shows the transmission spectra of the absorption edge is found around 510 nm.

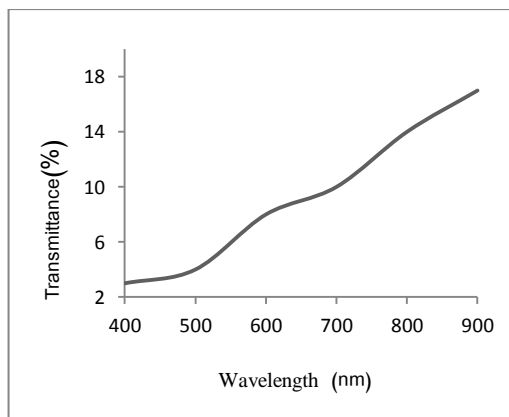


Fig.5: Transmittance spectrum of (NiO) thin film which prepared by chemical method and deposited by drop casting technique on glass.

Therefore using the fundamental relation of photon transmission and absorbance, the absorbance (A) is depend as the logarithm (base 10) of the reciprocal of the transmittance :

$$A = \log_{10} \frac{1}{T} \quad (4)$$

If T is the transmittance and A is the absorbance of the (NiO) thin film. The reflection of the film has been found by using relationship:

$$R + T + A = 1 \quad (5)$$

The reflection of the NiO thin film increases with increasing the wavelength above 510 nm .After that there is about 0.35 as shown in figure 6 due to increase in transmittance .

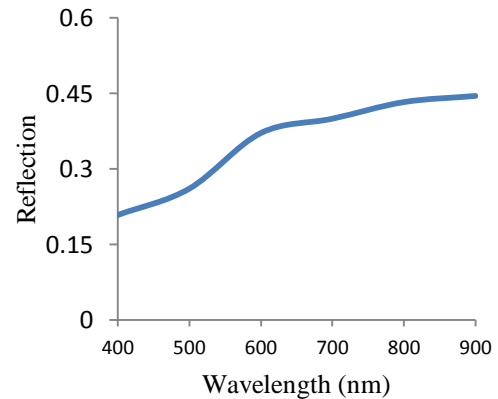


Fig.6: Reflection spectrum of (NiO) thin film which prepared by chemical method and deposited by drop casting technique on glass.

From the reflection R of the thin film, the refraction index can be calculated from the following relationship:

$$n = \frac{1 + \sqrt{R}}{1 - \sqrt{R}} \quad (6)$$

The refractive index (n) of the prepared NiO films have been calculated using equation 6, for a range of wavelength of 400 nm to 900 nm. The plot of wavelength versus n is shown in Fig. 7. the refractive index of the film remains almost equal through the visible region 400 nm to 510 nm with the value of 2.7 , then the refraction index increased above that.

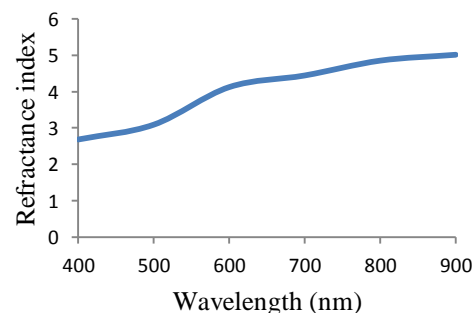


Fig.7: Refractance index spectrum of (NiO) thin film which prepared by chemical method and deposited by drop casting technique on glass.

The optical absorption coefficient α was evaluated by tauc relation $\alpha hv = A(hv - E_g)^n$ when $\alpha = 2.303 \frac{A}{t}$ where t is the film thickness, hv is the photon energy, $E_g = \frac{1240}{\lambda_{(nm)}}$ and $n = 0.5$ for allowed direct transition.

Plotting the graph between $(\alpha hv)^2$ versus photon energy (hv) gives the value of direct band gap. The extrapolation of the straight line to $(\alpha hv)^2 = 0$, gives the value of band gap, shown in figure 8. The optical band gap is 1.8 eV, in other word, the exactions wavelength ~ 688 nm. this results is very important to relieve that the (NiO) thin film can be use in solar cell device.

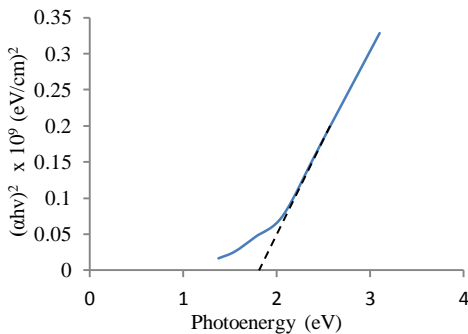


Fig.8: $(\alpha hv)^2$ versus photon energy plot of (NiO) thin film which prepared by chemical method and deposited by drop casting technique on glass.

The optical conductance is obtained using the relation,

$$\sigma = \alpha n c \epsilon_o = \frac{\alpha n c}{4\pi} \quad (7)$$

Where σ is the optical conductance, c is the velocity of the radiation in the space, n is the refractive index and α is the absorption coefficient. Figure 9 shows the relation between the optical conductivity and photon energy for NiO thin film. Also this figure shows the optical conductance increases from $(0.353 \times 10^{12} \text{ 1/sec})$ at 1.37eV to $(0.414 \times 10^{12} \text{ 1/sec})$ at 2eV then it is decreases after that.

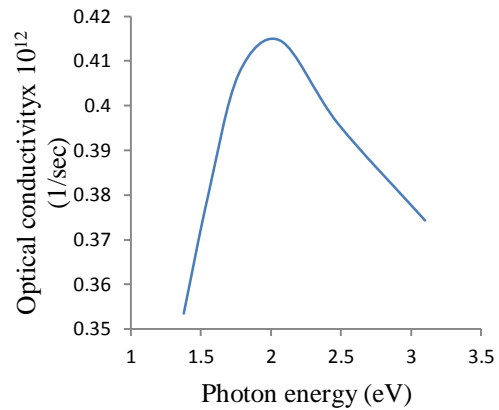


Fig.9: Optical conductivity of NiO thin film as a function of photon energy.

The extinction coefficient (k) can be determine by using the relation, $k = \frac{\alpha \lambda}{4\pi}$, where λ is the wavelength of light. The maximum value (peak) is 0.0215 and the minimum (valley) is about 0.0185 as shown in figure 10.

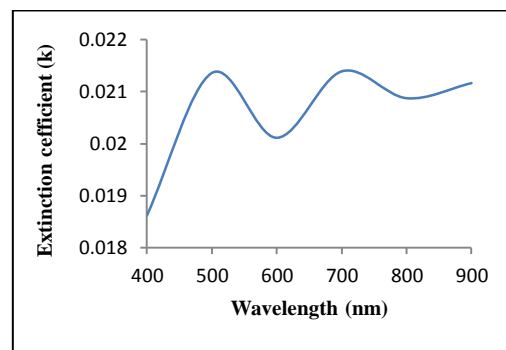


Fig.10: Extinction coefficient of NiO thin film as a function of photon energy.

Fourier Transform Infrared Spectro-scopy (FTIR) spectra was performed to the dried sample of magnetite using a FTIR – Shimadzu 8400 spectrophotometer in wave range of $(600 - 4200) \text{ cm}^{-1}$ with a resolution of 4 cm^{-1} .

Figure 11 shows the FTIR spectra of NiO nanoparticles, which showed several significant absorption peaks. The broad absorption band in the region of $(600-700) \text{ cm}^{-1}$ is assigned to Ni–O stretching vibration mode; the broadness of the absorption band indicates the nanocrystalline nature of the sample. The size of samples used in this study was much less than the bulks form NiO, so that NiO nanoparticles had its IR peak of Ni–O stretching

vibration and shifted to blue direction. Due to their quantum size effect and spherical nanostructures, the FTIR absorption of NiO nanoparticles is blue-shifted compared to that of the bulk form. In addition to Ni–O vibration, it could be seen from this figure that the broad absorption band centered at 3350 cm^{-1} is attributable to the band O–H stretching vibrations and the band near 1641.48 cm^{-1} is assigned to H–O–H bending vibrations mode. These indicate the presence of traces of water in the sample due to absorbed moisture. Furthermore, the band around 1045 cm^{-1} confirm the presence of C–O in the precursor and the band at 1375 cm^{-1} is primarily due to the banding vibration of ionic CO_3^{2-} while the vibration band of CH_2 occur at 2982 cm^{-1} .

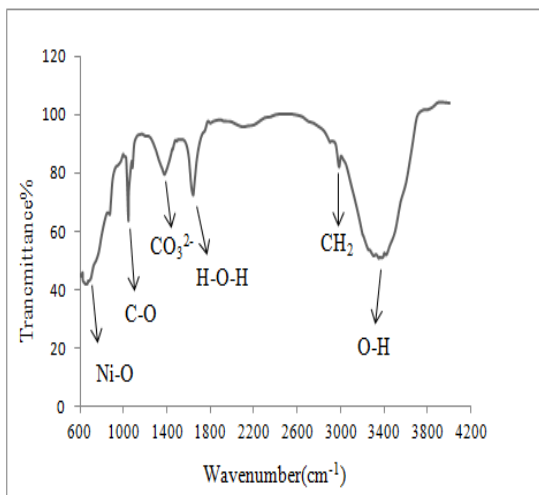


Fig.11: FTIR spectra NiO of thin film as a function of wavenumber .

Figure 12 shows the I-V dark characteristics in forward and reverse direction of Al / NiO / Si / Al heterojunction . The forward current of heterojunction is very small at voltage less than 2 V. This current is known as recombination current which occurs at low voltages only. It is generated when each electron excited from valence band to conductive band. The second region at high voltage represented the diffusion or bending region ,which depending on series resistance .In this region; the bias voltage can deliver electrons with enough energy to penetrate the barrier between the two sides of the junction.

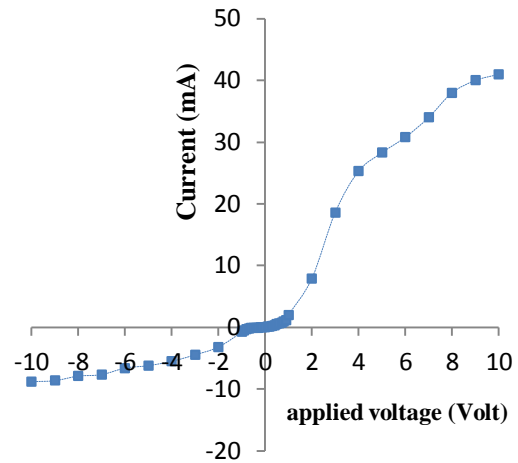


Fig. 12. I-V characteristic under forward reverse bias of the Al / NiO / Si / Al.

Figure 12 and 13 shows that the reversed current-voltage characteristics of the device measured in dark and the photocurrent under 41 W/cm^2 tungsten lamp illuminations. It can be seen that the reverse current value at a given voltage for Al/NiO/Si/Al heterojunction under illumination is higher than that in the dark and it can be seen from these figures that the current value at a given voltage for hetero-junction under illumination is higher than that in dark , this indicate that the light generated carrier – contributing photocurrent due to the production of electron –hole as a result of the light absorption. This behavior yield useful information on the electron-hole pairs, which are effectively generated in the junction by incident photons.

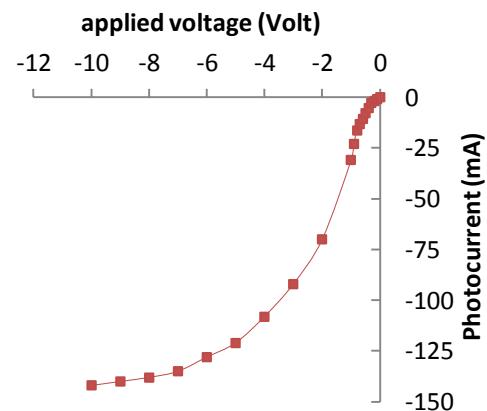


Fig.13: Illuminated (I-V) characteristic of Al/ NiO / Si / Al heterojunction

Fig. (14) Shows the I-V characteristics for NiO/Si. The measured short-circuit current, open-circuit voltage, fill factor and Efficiency are 2.2 μ A, 4.2 V, 0.26 and 8.4% respectively. All the results relieve that the sandwich structure Al/NiO/Si/Al could be used as a solar cell.

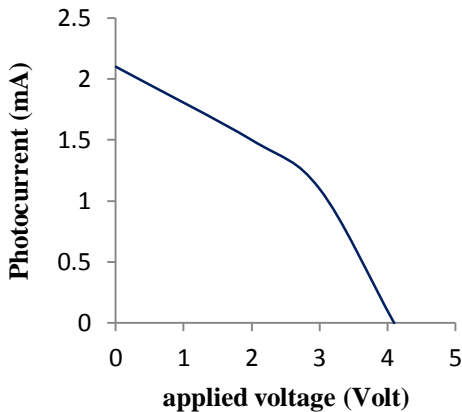


Fig. 14: I-V characteristics for Al/NiO/Si/Al heterojunction .

Conclusions

The synthesized (NiO) thin film by chemical method had minimum nanosized is around 95 nm and the optical properties revealed that the energy gap of (NiO) thin film indicated to the effect of quantum size. X-ray diffraction (XRD) exhibits spectrum that the (NiO) are polycrystalline. FTIR measurements shows that the absorption bond Ni–O bonds in the crystalline lattice of NiO .

The characteristics of Al/NiO/Si/Al shows good behavior of solar cell applications.

References

- [1] M. Guziewicz, *et al.*, "Electrical and optical properties of NiO films deposited by magnetron sputtering," *Optica Applicata*, vol. XLI, no. 2, pp. 431-440, 2011.
- [2] M. K. Lee and Y. T. Lai, "Characterization of transparent conducting p-type nickel oxide films grown by liquid phase deposition on glass," *J. Phys. D: Appl. Phys.*, vol. 46, no. 5, 2013.
- [3] P. S. Patil and L. D. Kadam, "Preparation and characterization of spray pyrolyzed nickel oxide (NiO) thin films," *Appl. Surf. Sci.*, vol. 199, pp. 211-221, 2002.
- [4] N. S. Das, B. Saha, R. Thapa, G. C. Das, and K. K. Chattopadhyay, "Band gap widening of nanocrystalline nickel oxide thin films via phosphorus doping," *Physica E*, 42, 5, (2010)1377-1382.
- [5] P. Mallick and N. C. Mishra, " Evolution of structure, micro-structure , electrical and magnetic properties of nickel oxide (NiO) with transition metal ion doping ,,"*American Journal of Materials Science* , 2, 3 (2012) 66-71.
- [6] L. Albertst and E. W. Lee, "Magnetostriction in antiferro-magnetic nickel oxide," *Proc. Phys. Soc.*, 78 (1961)728-733,.
- [7] M. Stamataki, D. Tsamakis, N. Brilis, I. Fasaki, A. Giannoudakos, and M. Kompitsas, "Hydrogen gas sensors based on PLD grown NiO thin film structures," *Phys. Stat. Sol. (A)*, 205, 8 (2008)2064-2068.
- [8] H. Kamal, E. K. Elmaghraby, S. A. Ali, and K. Abdel-Hady, "The electrochromic behavior of nickel oxide films sprayed at different preparative conditions," *Thin Solid Films*, 483 (2005)330-339.
- [9] W. Azelee, W. Abu Bakar, M. Yusuf Othman, R. Ali , C. Yong, and S. Toemen, "The investigation of active sites on nickel oxide based catalysts towards the in-situ reactions of methanation and desulfurization," *Modern Applied Science*, 3, 2,(2009) 35-43 ,.
- [10] J. Bandara and H. Weerasinghe, "Solid-state dye-sensitized solar cell with p-type NiO as a hole collector," *Sol. Energy Mater. Sol. Cells*, 85, 3 (2005) 385-390.
- [11] D. Y. Jiang, J. M. Qin, X. Wang, S. Gao, Q. C. Liang, and J. X. Zhao, "Optical properties of NiO thin films fabricated by electron beam evaporation," *Vacuum*, vol. 86, no. 8, (2012)1083-1086.
- [12] I. Hotovq, D. Buc, S. Hascik, "Characterization of NiO thin films prepared by reactive sputtering," *Vacuum*, 50 (1998)41-44.
- [13] E. Fujii, A. Tomozawa, H. Torii, and R. Takayama, "Preferred orientations of NiO films prepared by plasma-enhanced metalorganic chemical vapor

- deposition,” *Jpn. J. Appl. Phys.*, 35, (1996)328-330,.
- [14] I. Fasaki, A. Koutoulaki, M. Kompitsas, and C. Charitidis, “ Structural , electrical and mech-anical properties of NiO thin films grown by pulsed laser deposition,” *Appl. Surf. Sci.*, 257, 2, (2010)429-433,.
- [15] L. Cattin, B. A. Reguig, A. Khelil, M. Morsli, K. Benchouk, and J. C. Bernede, “Properties of NiO thin films deposited by chemical spray pyrolysis using different precursor solutions,” *Appl. Surf. Sci.*, 254, 18, (2008)5814-5821,.
- [16] X. H. Xia, J. P. Tu, J. Zhang, X. L. Wang, W. K. Zhang, and H. Huang, “Electrochromic properties of porous NiO thin films prepared by a chemical bath deposition,” *Sol. Energy Mater. Sol. Cells*, 92, 6, (2008) 628-633,.
- [17] E. Kashevsky, V.E. Agabekov, S.B. Kashevsky, K.A. Kekalo, E.Y. Manina, I.V. Prokhorov, V.S. Ulashchik, *Particuology* 6 (2008) 322.
- [18] Bragg W.L. *Nature*. **95** (1915) 561.